Chapter 5

Effect of Pressure on the Phonon Properties of III-V Phosphides

5.1 Introduction

On account of the explosion of information technology and computing, the late 20^{th} century has come to be regarded as the semiconductor age. The technological impact of these will be extremely crucial in order to develop new semiconductor devices. Structurally most semiconductors consist of a network of covalent bonds leading to an open crystal structure which, like water becomes denser on melting. They typically exhibit a series of high pressure phase transition to progressively denser structure and have thus become a paradigm for high pressure studies. In the specific case discussed here the group III- V compound semiconductors exhibits tetrahedral co-ordination under ambient conditions, typically in the diamond structure (zinc blende or wurtzite). The application of high pressure probes the physics of interatomic bonding extremely thoroughly. It gives rise to more dramatic changes in the physical properties of semiconductors that can be obtained through temperature variation alone, including band gap closure and metallization combined with the propensity of covalent materials to form long lived metastable structures. It is not therefore surprising that the high pressure properties of semi conductors are at the forefront of crystallographic study.

Like many III-V semiconductor compounds, the group III phosphides crystallizes in the cubic zinc blende structure, which closely resembles to diamond structure in these compounds. The group III elements have three electrons in the outermost shells with one electron occupying in the S state and other two in the P state. Similarly, group V element has two S electron and three P electrons in the outermost valance shell. Thus, the trivalent and pentavalent atoms constitute an average of four electron pair per atom. The binding

energy of these compounds is to some extent homopolar as in the case of IV group elements. However, as a result of comparatively large electronegativity of the fifth group elements, there is a small ionic contribution to the binding energy. The covalent character of the bond in these compounds is consistent with the fact that the interatomic distances are approximately equal to the covalent radii of the atoms, while sum of the ionic radii is considerably small. This fact makes them partially covalent.

However, the understanding of the interatomic forces and the study of the phonon properties of compound semiconductors requires adequate knowledge of their structural as well as physical properties. Since pioneering work of Mitra et al [1], pressure dependence of phonon modes in semi conductor have been investigated by Raman scattering [2,3,4], as Raman scattering (RS) is probably the most amenable method from among the various available techniques. Cardona and his co-workers [3,5-9] used RS to observe the effect of pressure on the lattice dynamics of III-V compounds up to phase transition pressure, in which Raman scattering reveals phase transition as discontinuities in phonon frequencies or intensity of phonon peaks. Until very recently, inelastic scattering could not be performed under sufficiently high pressure to measure shifts with sufficient precision. However, recent developments in these techniques removed these drawbacks [10-12]. In a recent work, Polian and Grimsditch [13] using Brillouin scattering measurements measured the pressure dependence of GaP up to 15 GPa using a diamond anavil cell. Thus modern techniques helped experimentalist to perform their job by developing different methods to generate high pressure and its measurements.

On the other hand, very few attempts have been made to investigate high pressure phonon properties of semi conductors using model theories [14-16]. However, recently it has become possible to compute with a great accuracy an important number of structural and electronic properties of solids from ab intio calculations. Among the quantities calculated from this, kind of studies are the crystal structure, lattice constant, bulk and shear moduli and other static and dynamic properties of materials. This kind of development in computer simulation has opened up possibilities to predict properties of the solids, which were previously inaccessible for experiments. Recently, the method of

calculation has been developed by Nielsen and Martin [17] and allows to calculate elastic constants using direct calculations of microscopic stress and force on the atoms. These facts motivated us to study phonon properties of the III- phosphide through the Brillouin zone at ambient and at high pressure which is close to their phase transition pressure. In the present chapter, we report the results of our investigations on pressure dependent phonon dispersion curves, phonon density of states, mode Grüneisen parameters and specific heat for three III- phosphides namely InP, GaP and BP and one antimonide namely GaSb by using rigid ion model as well as deformation bond approximation model (DBA) discussed in chapter 3. In addition we have also reported variation in the phonon frequencies at different points in the BZ with pressure for mentioned phosphides and GaSb. We have also performed study of variation of LO-TO splitting at Γ-point with pressure. In section 2, we describe theoretical consideration and determination of parameters. Section 3 gives the idea about the results and discussion of the results followed by conclusion in section 4.

5.2 The Present Calculation

To perform the comprehensive study of phonon properties of III- phosphides we have used two model namely rigid ion model (RIM) and deformation bond approximation model (DBA) discussed in chapter 3. Details about RIM and optimization of the model parameters at high pressure have already been presented in chapter 4. The deformation bond approximation model (DBA) also has been explained in detail in chapter 3 and the parameters at ambient and high pressure have been determined by the same methodology as described in chapter 4 (See section 4.2) for rigid ion model. However, some silent features of DBA is described below.

A look at the literature reveals that deformation bond approximation is most suitable to interpret the covalent nature and explain the phonon properties of III-V compounds. This fact is well supported by Kunc et al [18] who performed extensive calculations of PDC of several compound semiconductors at ambient pressure. Two

simple assumptions for deformation dipole model, which in general do not affect the generalities of the model, make it simpler and handy. The simplification consists:

(i) to reduce the number of independent "deformabilities" and

(ii) to neglect the "non local electric polariziabilities".

The above two general assumptions on the general deformation-dipole model are called the deformable bond approximations (DBA) [19]. In the case of Zinc blende structure, it represents a model with 14 independent parameters: "static ionic charge", two "deformabilities", two "local electric polariziabilities", and 10 short range coupling parameters extending to second neighbors. The model parameters are determined in the same way as discussed in chapter 4 for RIM. The model parameters obtained by the methodology discussed above are presented in Table 2. While the input parameters used to obtain the model parameters are presented in Table 1. We plot first neighbor force constant for zinc blende InP, GaP, BP and GaSb compound semiconductors in figure 1.

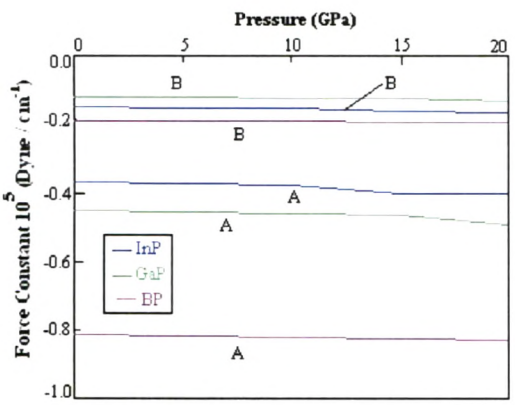

Figure 1 (a): Force constant (A and B) as a function of pressure for InP, GaP and BP.

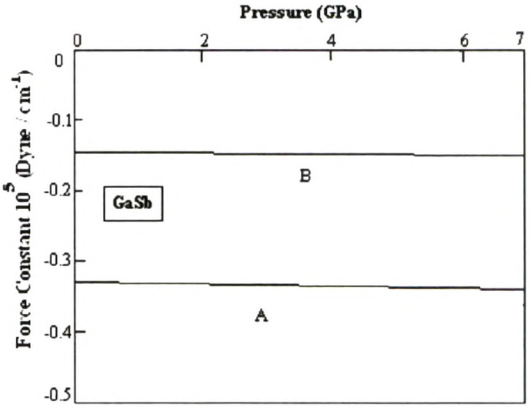

Figure 1 (b): Force constant (A and B) as a function of pressure for GaSb.

Table 1: RIM input parameters for III-Phosphides and GaSb. Elastic constants C_{ij} (x 10^{11} dyne / cm^2).

Input Parameters for Phosphides and GaSb				
Parameter	**InP**	**GaP**	**BP**	**GaSb**
C_{11}	10.11	14.12	31.50	8.850
C_{12}	5.610	6.250	10.00	4.640
C_{44}	4.560	7.050	16.00	4.330
M_1 (amu)	114.8	69.72	10.81	69.72
M_2 (amu)	30.97	30.97	30.97	121.7
a (Å)	5.870	5.450	4.538	6.120
ω_{LO} (cm^{-1})	345	403	799	240
ω_{TO} (cm^{-1})	306	365	807	237

Table 2 (a): Calculated RIM parameters (10^5 dyne / cm) for zinc blende InP. Z is a proton charge. The lattice parameter a is in Å.

RIM Parameters for InP					
Parameters	**0 GPa**	**5 GPa**	**10 GPa**	**15 GPa**	**20 GPa**
A	-0.3700	-0.3744	-0.3770	-0.4019	-0.4036
B	-0.1500	-0.1518	-0.1529	-0.163	-0.1637
C1	-0.0600	-0.0607	-0.0611	-0.0651	-0.0654
D1	-0.0900	-0.0911	-0.0917	-0.0977	-0.0981
E1	0.0912	0.0923	0.0929	0.0990	0.0994
F1	0.1925	0.1965	0.2006	0.2048	0.2091
C2	-0.0260	-0.0263	-0.0265	-0.0282	-0.0283
D2	-0.0010	-0.0010	-0.0010	-0.0011	-0.0011
E2	0.0034	0.0034	0.0034	0.0036	0.0036
F2	-0.0325	-0.0329	-0.0331	-0.0353	-0.0355
Z	0.8000	0.7905	0.7850	0.7332	0.7300
a	5.8700	5.8007	5.7603	5.3802	5.3568

Table 2 (b): Calculated RIM parameters (10^5 dyne / cm) for zinc blende GaP. Z is a proton charge. The lattice parameter a is in Å.

RIM Parameters for GaP					
Parameters	**0 GPa**	**5 GPa**	**10 GPa**	**15 GPa**	**20 GPa**
A	-0.4500	-0.4561	-0.4601	-0.4634	-0.4912
B	-0.1200	-0.1216	-0.1227	-0.1236	-0.1310
C1	-0.0430	-0.0435	-0.0440	-0.0443	-0.0469
D1	-0.0700	-0.0709	-0.0715	-0.0720	-0.0763
E1	0.0912	0.0924	0.0932	0.0939	0.0995
F1	0.2005	0.2060	0.2117	0.2175	0.2400
C2	-0.0345	-0.0350	-0.0353	-0.0355	-0.0376
D2	-0.0401	-0.0406	-0.0410	-0.0413	-0.0438
E2	0.0034	0.0034	0.0034	0.0035	0.0037
F2	-0.0350	-0.0355	-0.0358	-0.0361	-0.0383
Z	0.7500	0.7398	0.7334	0.7281	0.6844
a	5.4500	5.3763	5.3293	5.2910	4.9736

Table 2 (c): Calculated RIM parameters (10^5 dyne / cm) (A,B, Ci, Di, Fi, i=1,2) for zinc blende BP. Z is a proton charge. The lattice parameter a is in Å.

RIM Parameters for BP					
Parameters	**0 GPa**	**5 GPa**	**10 GPa**	**15 GPa**	**20 GPa**
A	-0.8100	-0.8150	-0.8200	-0.8246	-0.8285
B	-0.1900	-0.1912	-0.1924	-0.1935	-0.1944
C1	-0.0454	-0.0457	-0.0460	-0.0463	-0.0465
D1	0.0300	0.0302	0.0304	0.0306	0.0307
E1	0.0912	0.0918	0.0924	0.0929	0.0933
F1	0.0475	0.1200	0.2000	0.2400	0.2700
C2	-0.1014	-0.1020	-0.1026	-0.1032	-0.1037
D2	-0.2436	-0.2451	-0.2466	-0.2480	-0.2492
E2	0.0034	0.0034	0.0034	0.0034	0.0034
F2	0.2805	0.2822	0.2839	0.2855	0.2868
Z	0.6250	0.6211	0.6173	0.6138	0.6109
a	4.53800	4.5099	4.4821	4.4567	4.4357

Table 2 (d): Calculated RIM parameters (10^5 dyne / cm) (A,B, Ci, Di, Fi, i=1,2) for zinc blende GaSb. Z is a proton charge. The lattice parameter a is in Å.

RIM Parameters for GaSb					
Parameter	**0 GPa**	**2 GPa**	**4 GPa**	**6 GPa**	**7 GPa**
A	-0.3516	-0.3544	-0.3572	-0.3601	-0.3615
B	-0.1450	-0.1462	-0.1474	-0.1486	-0.1492
C_1	-0.0238	-0.0240	-0.0242	-0.0244	-0.0245
D_1	-0.0338	-0.0341	-0.0344	-0.0347	-0.0348
E_1	0.0252	0.0254	0.0256	0.0258	0.0259
F_1	-0.0942	-0.0950	-0.0958	-0.0966	-0.0970
C_2	0.1812	0.1827	0.1842	0.1857	0.1864
D_2	0.0034	0.0034	0.0034	0.0035	0.0035
E_2	-0.0215	-0.0217	-0.0219	-0.0221	-0.0222
F_2	0.1505	0.1517	0.1529	0.1541	0.1547
Z	0.6000	0.5950	0.5900	0.5850	0.5820
a	6.1200	6.0700	6.0200	5.9700	5.9500

Table 3 (a): Calculated DBA parameters (10^5 dyne / cm)for InP. Z is proton charge.

DBA Parameters for InP		
Parameters	**0 GPa**	**5 GPa**
A	-0.4800	-0.4865
B	-0.1200	-0.1216
C_1	-0.0375	-0.0380
D_1	-0.1000	-0.1014
E_1	0.0912	0.0924
F_1	0.1550	0.1571
C_2	-0.0345	-0.0350
D_2	-0.0700	-0.0709
F_2	-0.0700	-0.0709
α_1	0.1410	0.1429
α_2	3.500	3.5473
γ_1	0.1940	0.1966
γ_2	0.3951	0.4004
Z	0.0545	0.0552

Table 3 (b): Calculated DBA parameters (10^5 dyne / cm) for GaP. Z a proton charge..

DBA Parameters for GaP					
Parameters	**0 GPa**	**5 GPa**	**10 GPa**	**15 GPa**	**20 GPa**
A	-0.4800	-0.4865	-0.4907	-0.4942	-0.5238
B	-0.1200	-0.1216	-0.1227	-0.1236	-0.1310
C_1	-0.0375	-0.0380	-0.0383	-0.0386	-0.0409
D_1	-0.1000	-0.1014	-0.1023	-0.0130	-0.1092
E_1	0.0912	0.0924	0.0932	0.0939	0.0995
F_1	0.1550	0.1571	0.1585	0.1596	0.1692
C_2	-0.0345	-0.0350	-0.0353	-0.0355	-0.0376
D_2	-0.0700	-0.0709	-0.0715	-0.0720	-0.0763
F_2	-0.0700	-0.0709	-0.0715	-0.0720	-0.0763
α_1	0.1410	0.1429	0.1441	0.1451	0.1583
α_2	3.500	3.5473	3.5783	3.6040	3.8202
γ_1	0.1940	0.1966	0.1983	0.1997	0.2117
γ_2	0.3951	0.4004	0.4039	0.4122	0.4369
Z	0.0545	0.0552	0.0557	0.0561	0.0595

Table 3 (c): Calculated DBA parameters (10^5 dyne / cm) for BP. Z is a proton charge.

DBA Parameters for BP					
Parameters	**0 GPa**	**5 GPa**	**10 GPa**	**15 GPa**	**20 GPa**
A	-0.8500	-0.8552	-0.8605	-0.8654	-0.8694
B	-0.0500	0.1526	-0.0506	-0.0508	-0.0511
C_1	-0.0325	-0.0327	-0.0329	-0.0329	-0.0312
D_1	0.0300	0.0302	0.0304	0.0306	0.0307
E_1	0.0912	0.0917	0.0923	0.0928	0.0933
F_1	-0.0200	-0.0201	-0.0202	-0.0203	-0.0204
C_2	-0.1014	-0.1020	-0.1026	-0.1032	-0.1037
D_2	-0.2900	-0.2918	-0.2963	-0.298	-0.2966
F_2	0.2805	0.2822	0.2840	0.0286	0.2869
α_1	0.1410	0.1420	0.1427	0.1435	0.1442
α_2	2.5000	2.5154	2.5308	2.5451	2.5570
γ_1	0.1940	0.1952	0.1964	0.1975	0.1984
γ_2	0.2500	0.2515	0.2531	0.2545	0.2557
Z	0.0545	0.0548	0.0552	0.0555	0.0557

Table 3 (d): Calculated DBA parameters (10^5 dyne / cm) for GaSb. Z is a proton charge.

DBA Parameters for GaSb						
Parameter	**0 GPa**	**2 GPa**	**4 GPa**	**6 GPa**	**7 GPa**	**8 GPa**
A	-0.3716	-0.3745	-0.3775	-0.3805	-0.3820	-0.3835
B	-0.1120	-0.1206	-0.1299	-0.1399	-0.1453	-0.1509
C_1	-0.0238	-0.0240	-0.0242	-0.0244	-0.0245	-0.0246
D_1	0.0252	0.0254	0.0256	0.0258	0.0259	0.0260
E_1	0.0912	0.0919	0.0927	0.0935	0.0939	0.0943
F_1	-0.0303	-0.0306	-0.0309	-0.0312	-0.0313	-0.0314
C_2	-0.0238	-0.0240	-0.0242	-0.0244	-0.0245	-0.0246
D_2	-0.0942	-0.0950	-0.0958	-0.0966	-0.0970	-0.0974
F_2	0.1375	0.1386	0.1397	0.1408	0.1414	0.1420
α_1	0.1410	0.1421	0.1432	0.1443	0.1449	0.1455
α_2	8.1321	8.1972	8.2628	8.3289	8.3622	8.3956
γ_1	-0.0940	-0.0948	-0.0955	-0.0963	-0.0967	-0.0971
γ_2	0.3951	0.3983	0.4012	0.4044	0.4060	0.4076
Z	0.0545	0.0549	0.0553	0.0557	0.0559	0.0561

5.3 Result and Discussion

5.3.1 Phonon dispersion curves

We present the results of theoretical study on the phonon dispersion curves using two models namely rigid ion model (RIM) and deformation bond approximation model (DBA) for InP, GaP, BP and Gasb. This comprehensive study is carried out to clarify the mechanism of the pressure induced phase transition in these compounds nearly close to phase transition pressure. The results on the phonon dispersion curves for InP, GaP, BP and Gasb are discussed in detail as below:

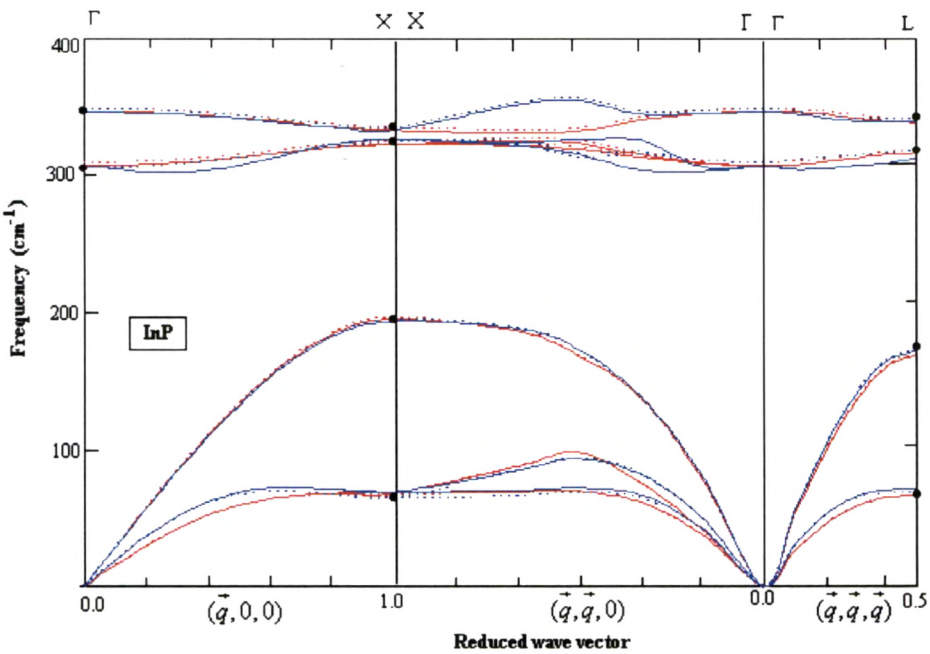

Figure 2 (a): Phonon dispersion curves for zinc blende InP semiconductor. ___ and --- represents ambient and 20 GPa RIM calculations whereas __ and --- represents ambient at 20 GPa DBA calculations. Filled circles present experimental data. [Ref. 33-34].

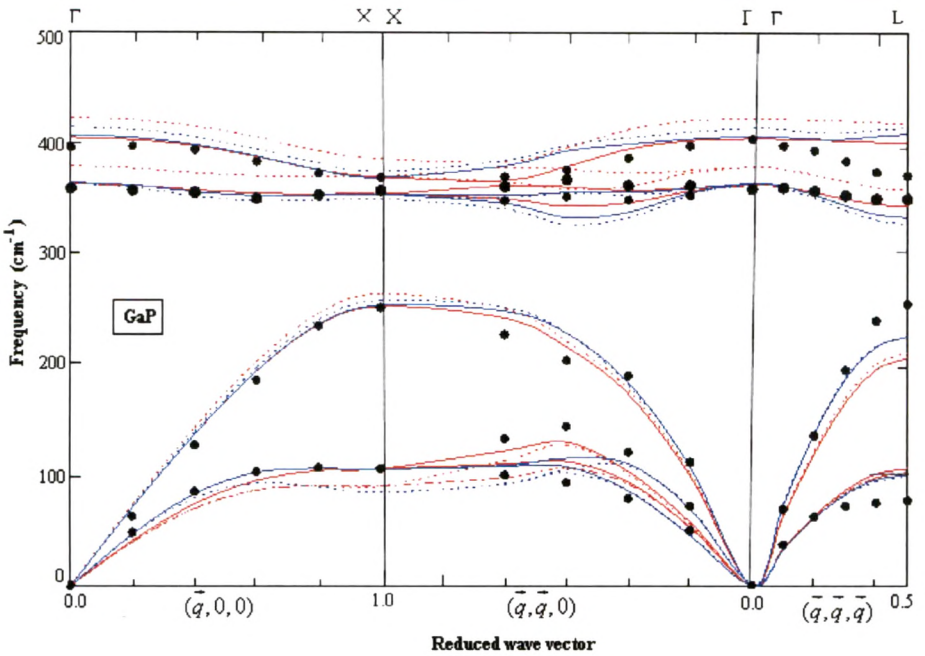

Figure 2 (b): Phonon dispersion curves for zinc blende GaP semiconductor. ___ and --- represents ambient and 20 GPa RIM calculations whereas __ and --- represents ambient and 20 GPa DBA calculations. Filled circles present experimental data. [Ref.22]

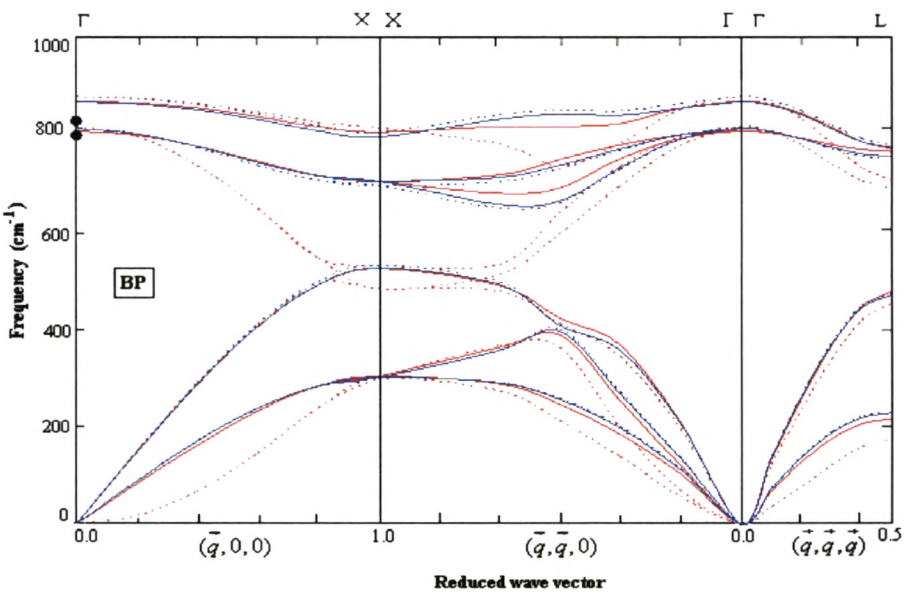

Figure 2 (c): phonon dispersion for zinc blende BP semiconductor. ___ and --- represents ambient and 20 GPa RIM calculations whereas __ and --- represents ambient at 20 GPa DBA calculations. Filled circles present experimental data. [Ref. 28].

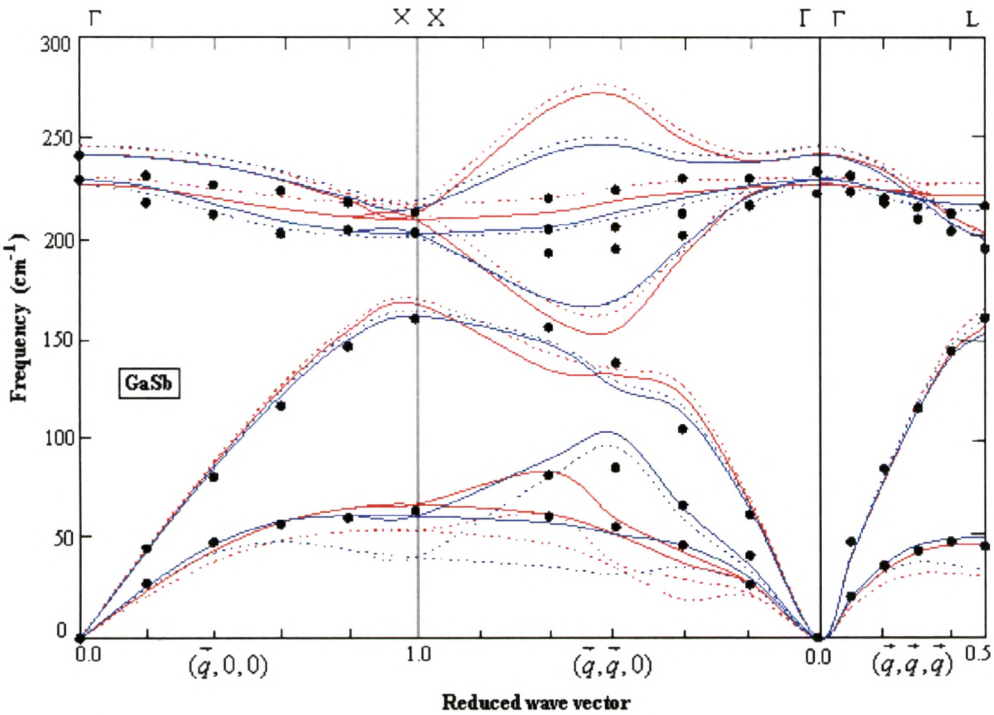

Figure 2 (d): phonon dispersion curves for zinc blende GaSb semiconductor. ___ and --- represents ambient and 8 GPa RIM calculations whereas ___ and --- represents DBA and 8 GPa calculations. Filled circles present experimental data. [Ref.29]

In ambient conditions, group III- phosphides crystallize in the cubic zinc blende structure. Under hydrostatic pressure, the low pressure phase is destabilized and structural phase transition to a high coordination phase appears. The phase transition pressure for GaP, InP and BP is respectively 20 GPa, 10GPa and 150 GPa [20] respectively, while for GaSb it is 8.5 GPa [30-32]. The phonon dispersion curves for InP, GaP, BP and GaSb are shown in figure 2(a-d).

Even though we have performed the high pressure study for all these materials at several different pressures, we have plotted phonon dispersion curves only at ambient and at a pressure, which is close to its phase transition pressure. The results with both RIM and DBA are plotted. These curves reveals all genuine characteristics of III-V compound semiconductors such as less dispersive behavior of optical branch particularly in $(\vec{q},0,0)$ and $(\vec{q},\vec{q},\vec{q})$, almost flat TO modes, increase in LO, TO and LA with pressure whereas

decrease in TA with pressure (see figure 3-6). Here we summarize some of the silent features found in the phonon behavior.

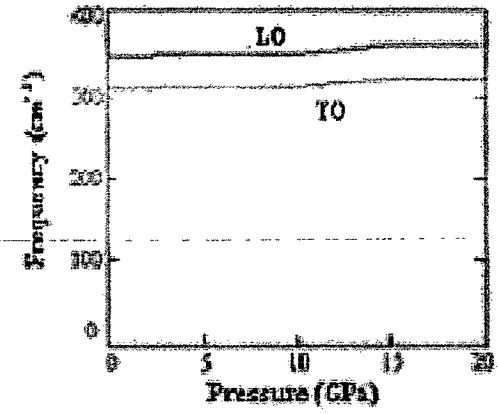

(a)

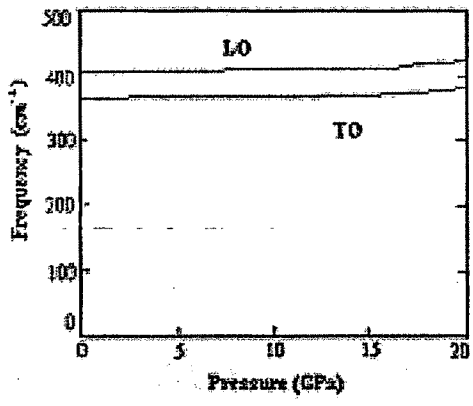

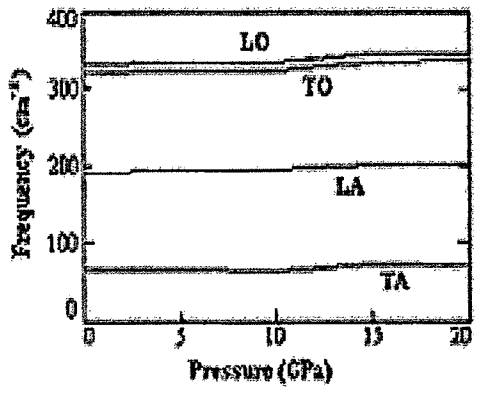

(b)

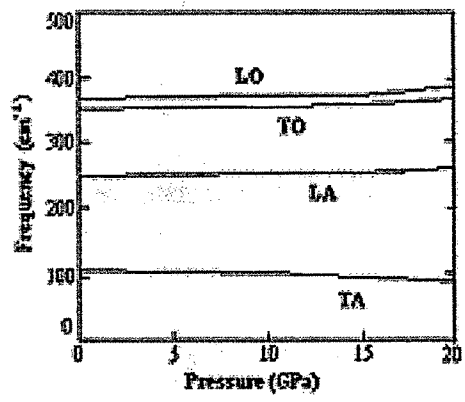

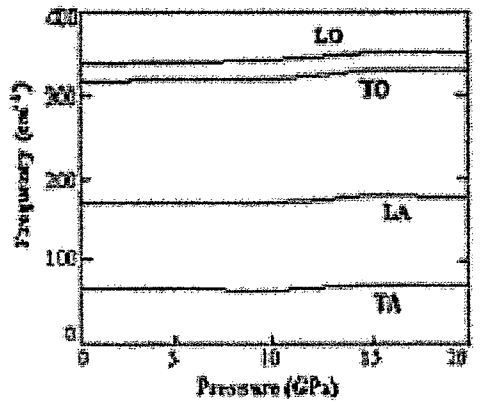

(c)

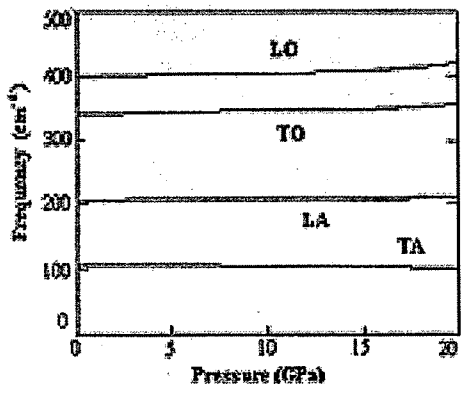

Figure 3: Variation of (a) ω_{LO}, ω_{TO} at Γ -point (b)ω_{LO}, ω_{TO}, ω_{LA} and ω_{TA} at X , and (c) ω_{LO}, ω_{TO}, ω_{LA} and ω_{TA} at L with pressure for InP.

Figure 4: Variation of (a) ω_{LO}, ω_{TO} at Γ - point (b)ω_{LO}, ω_{TO}, ω_{LA} and ω_{TA} at X , and (c) ω_{LO}, ω_{TO},ω_{LA} and ω_{TA} at L with pressure for GaP.

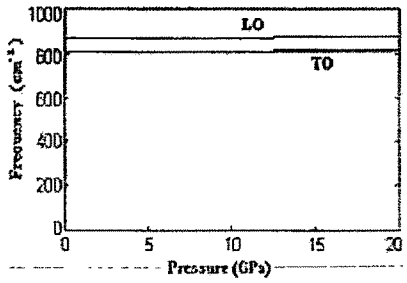

(a)

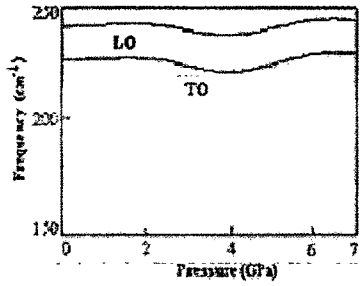

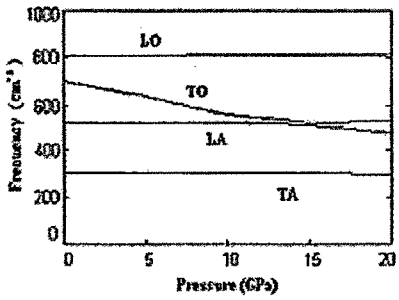

(b)

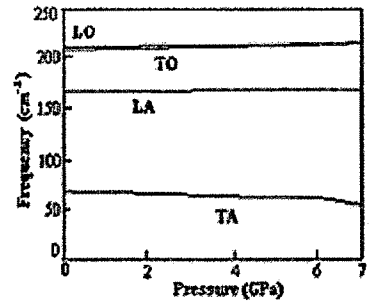

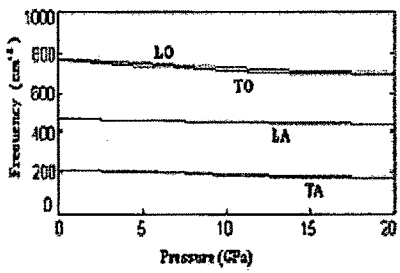

(c)

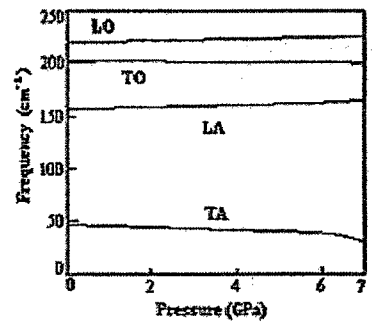

Figure 5: Variation of (a) ω_{LO}, ω_{TO} at Γ -point (b)ω_{LO}, ω_{TO}, ω_{LA} and ω_{TA} at X , and (c) ω_{LO}, ω_{TO}, ω_{LA} and ω_{TA} at L with pressure

Figure 6: Variation of (a) ω_{LO}, ω_{TO} at Γ -point (b)ω_{LO}, ω_{TO}, ω_{LA} and ω_{TA} at X , and (c) ω_{LO}, ω_{TO}, ω_{LA} and ω_{TA} at L with pressure for GaSb.

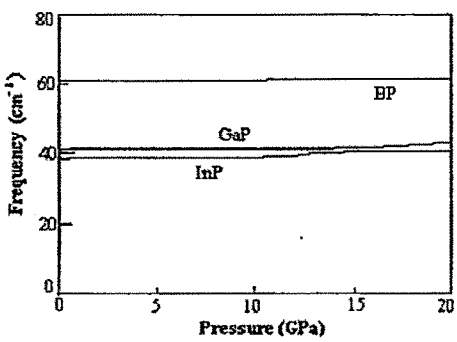

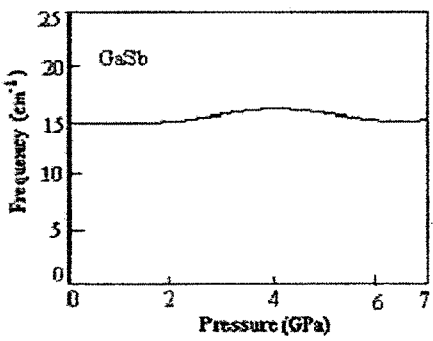

Figure 7 (a): Pressure variation for ω_{LO} - ω_{TO} at Γ- point for InP, GaP and BP and GaSb.

- ❖ For the III-P, optical-acoustic band gap decreases with increase in the anion to cation mass ratio for sequence InP → GaP → BP similar to the III-nitrides.
- ❖ As far as the comparison between two different models is concerned the DBA is more successful in predicting the gross features of phonon dispersion curves. This is due to the fact that the DBA incorporates the proper account of polarizability and force in the tetrahedraly bonded compound semiconductors.
- ❖ A satisfactory agreement of $\omega_j(\bar{q})$ both for P = 0 [21-25] and $P \neq 0$ [3, 5-9] in the above figures is quite eminent. The energies of the zone boundary and near zone boundary TA phonons decrease with pressure. This in consistent with the behavior of other III-V compound semiconductors which is confirmed by PDC of GaSb. The energies of LA (X) and LA (L) increases with pressure in agreement with II-VI compound semiconductors [32]. The optical phonons at Γ point in Brillouin Zone shifts in higher energies with pressure. As TO (Γ) shifts faster than LO (Γ), splitting ω_{LO} - ω_{TO} decrease with pressure which affect e^*_T. Thus this shows that as pressure increases, interatomic distance shortens causing stiffening in the short range forces and results in less transfer of charge for compressed crystal and decreasing e^*_T. A remarkable feature is observed that the TO phonon modes of InP shows softening throughout the BZ with the increase of pressure which may be due to the fact that proper parameters have not been obtained. However, we can not make any comment due to non-availability of experiment points.

5.3.2 Phonon Density of States

In addition to phonon dispersion curves for III-phosphides and GaSb, we have calculated one phonon density of states for these compounds at both ambient and high pressure with RIM as well as DBA. The calculated one phonon density of states is shown in figures 8(a-d). It is evident from the density of states that as pressure increases there is pronounced shift of the peaks and charge in the intensity of peaks. It can be seen in the case of InP and GaP that there is a shift of peaks towards lower energy side in the

acoustic phonon region, the peaks of optical phonon region shift towards higher energy side for both model with pressure. As far as the comparison of two model are concerned, the height of peaks in DBA calculation is lower than the RIM calculation for both compounds. There are distinct gaps in the phonon spectra which are reduced. Similar features are also observed in the case of BP and GaSb. In these systems also, BP while RIM shows shift towards lower side for almost all peaks the DBA shows the behavior of peaks similar to other phosphides. The spectra is continuous i.e. there is no gap in the both calculations. For GaSb both models are successful in showing the shift of peaks under pressure as observed for other compounds. But the range of phonon frequency in the case of RIM covers more region that is why the peaks seen prominently on both sides of the spectrum. The continuous peaks throughout the spectra are consistent with the dispersion curves.

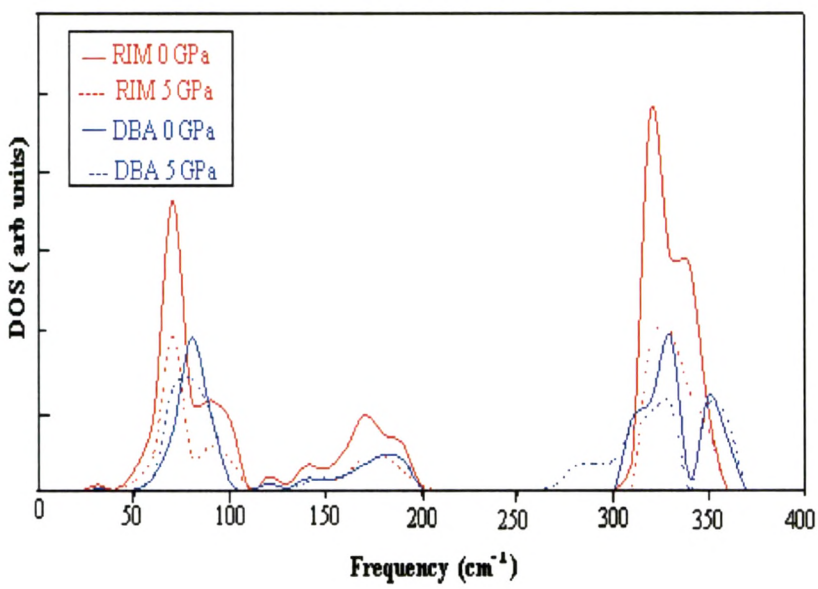

Figure 8 (a): One phonon density of states for InP.

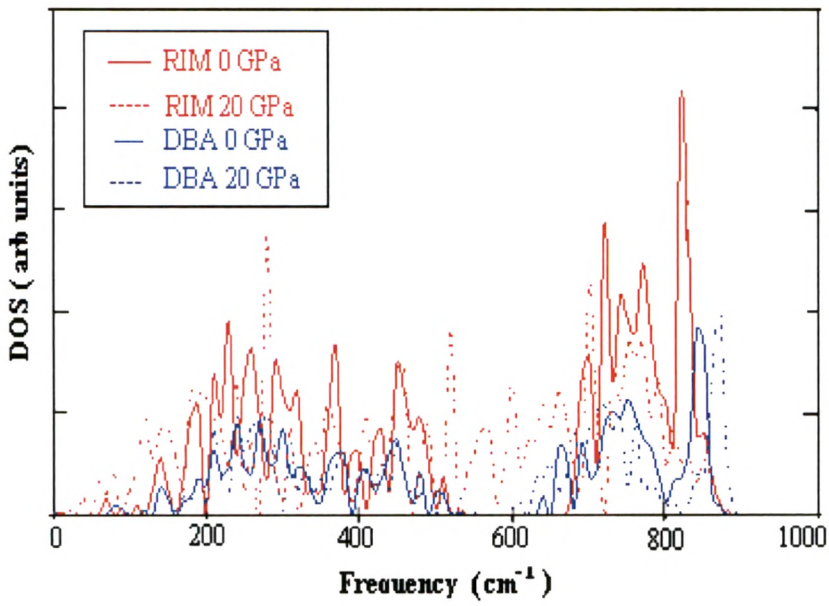

Figure 8 (b): One phonon density of states for GaP.

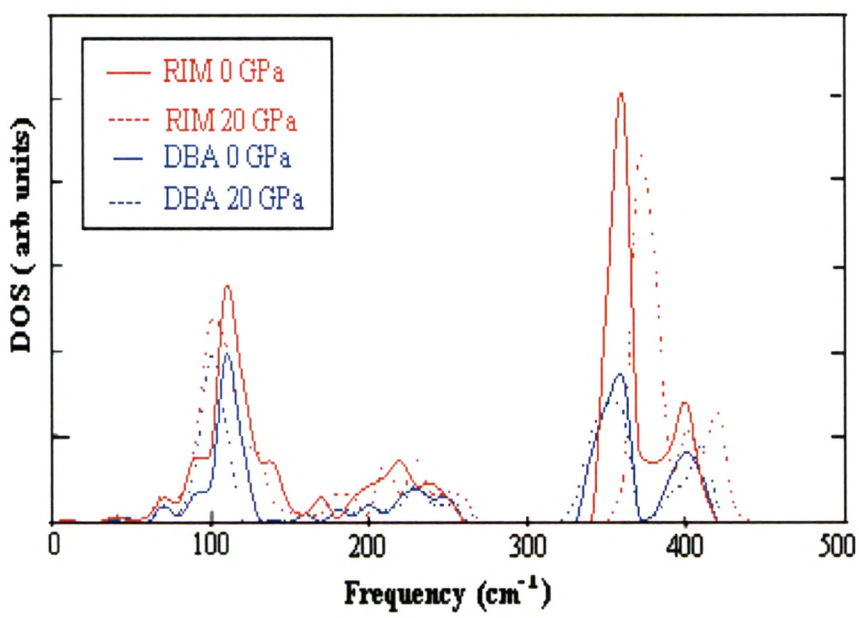

Figure 8 (c): One phonon density of states for BP.

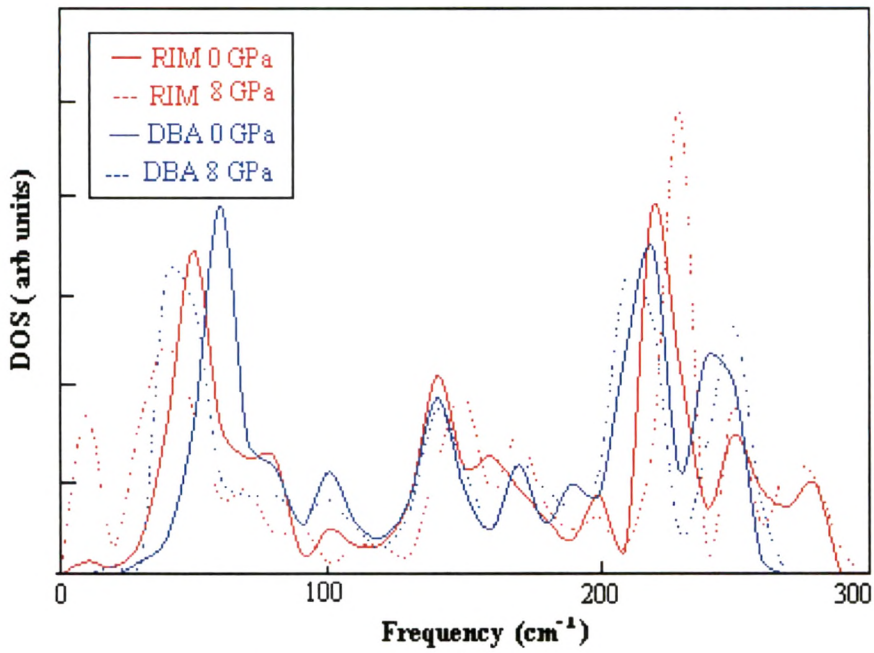

Figure 8 (d): One phonon density of states for GaSb.

5.3.3 Mode Grüneisen Parameters

As discussed in chapter 4 , if the knowledge of mode Grüneisen parameter is known in a solid for all branches through out the BZ, the responsible phonon modes for driving the transition or modes can be found along with the determination of thermal expansion. The calculated values of the $\omega_i(\vec{q})$ and $\frac{d\omega_i(\vec{q})}{dP}$ as a function of wave vector $\vec{q}$ through out the Brillouin Zone are used to study the variation of the mode Grüneisen parameter $\gamma_i(\vec{q})$. The results along $(\vec{q},0,0),(\vec{q},\vec{q},0)$ and $(\vec{q},\vec{q},\vec{q})$ for all four III-V phosphides are displayed in figures 9(a-d).

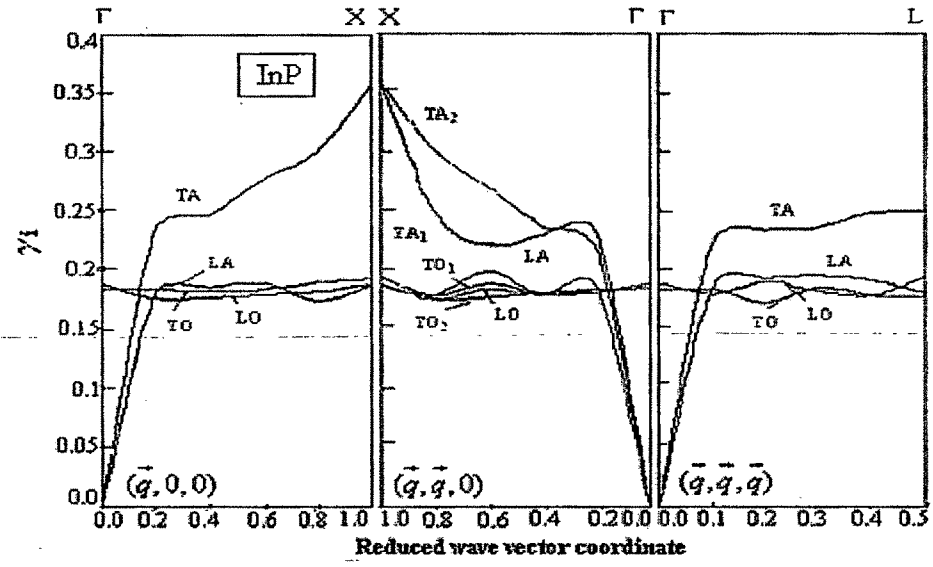

Figure 9 (a): Calculated mode Grüneisen parameter along high symmetry directions for InP.

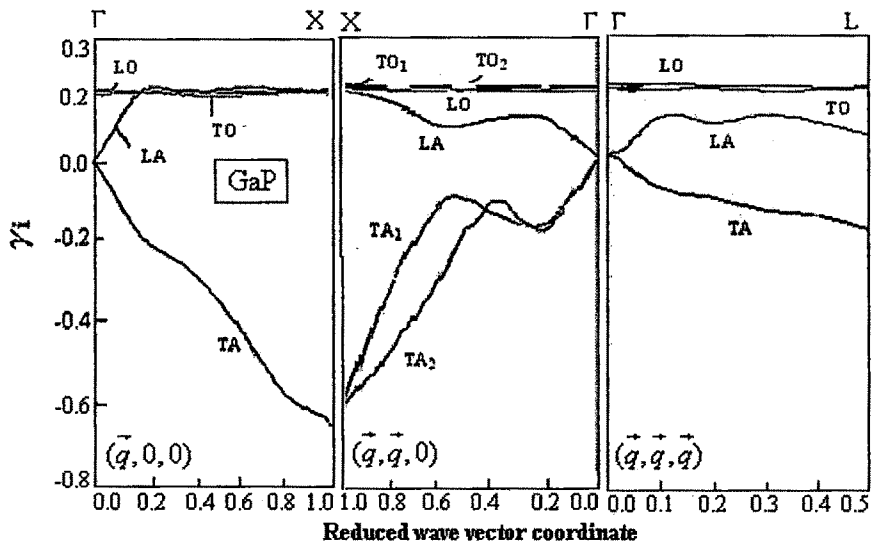

Figure 9 (b): Calculated mode Grüneisen parameter along high symmetry directions for GaP.

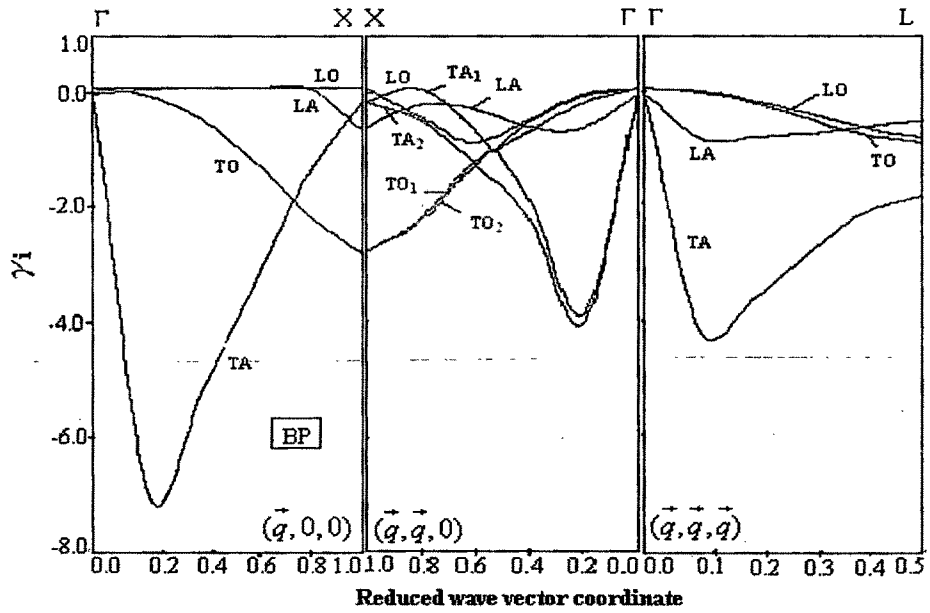

Figure 9 (c): Calculated mode Grüneisen parameter along high symmetry directions for BP.

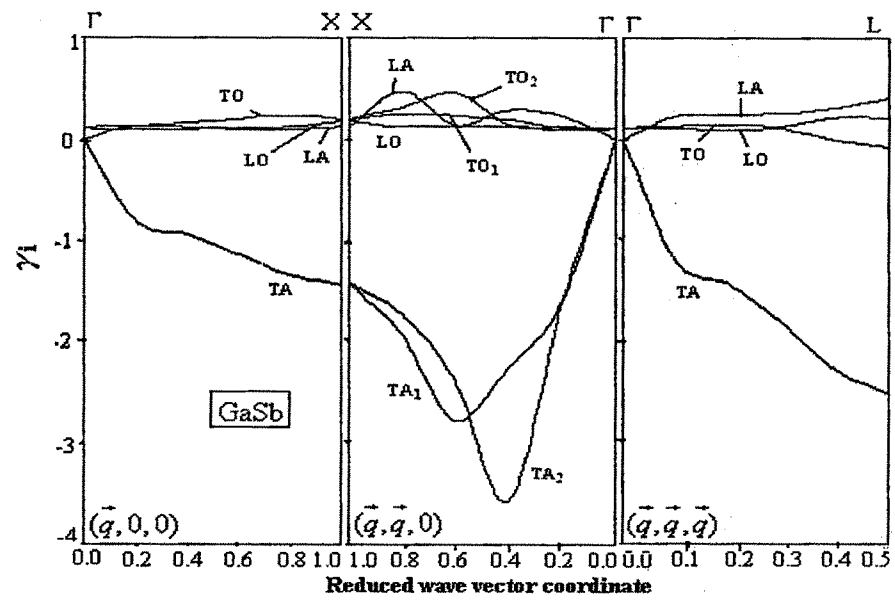

Figure 9 (d): Calculated mode Grüneisen parameter along high symmetry directions for GaSb.

These figures reveal that mode Grüneisen for the TA branches in III-phosphides and GaSb are negative while for all other branches they are almost positive, but with very small value. This may be due to the compensation between central and non central forces in these compounds similar to III-nitrides. Also, these indicates that the lattice softening of the TA phonons is primarily responsible for the observed phase transition in these compounds.

5.3.4 Specific Heat at Constant Volume

The lattice specific heat at constant volume C_v at ambient and at high pressure has been calculated for the InP, GaP, BP and GaSb and presented in Table 3. Here we just present these values only calculated by using one model namely deformation bond approximation model as the trend with pressure for both models is similar. It is seen from the Table 3, that the C_v increase with the increase in pressure for all four considered compounds, which is quite obvious due to the modification in phonon spectra under application of pressure.

Table 3: Specific heat (Joule/ mole-K) for InP, GaP and BP with pressure.

Specific Heat at Pressure (Joule/ mole. K)			
Pressure	**InP**	**GaP**	**BP**
0 GPa	270.63	193.76	50.5
5 GPa	270.65	193.77	56.7
10 GPa	272.37	195.75	67.26
15 GPa	255.92	198.15	74.95
20 GPa	258.22	198.35	83

5.4 Conclusions

In the present chapter, a comprehensive lattice dynamical study of InP, GaP, BP, and GaSb under pressure is reported by using two lattice dynamical model theories namely rigid ion and deformation bond approximation models. It is observed that the energies of the optical phonons and longitudinal acoustic phonons increase with pressure, while the transverse acoustic phonon frequency decreases for all considered compounds.

The phonon density of states show pronounced shift in the frequency spectra with pressure. The gap in the phonon spectra at both ambient and high pressure decreases as the mass ratio decreases. The mode Gruneisen parameter indicates that the TA phonon modes have negative values and responsible for the lattice softening. The lattice specific heat at constant volume, C_V increases with pressure for all compounds.

References

1. S S Mitra, *Phys. Rev.* **186**, 942 (1969).

2. B A Weinstein and R Zalleh, *in Light Scattering in Solids* **IV**, edited by M Cardona and G Guntherodt, 463 (Springer-Verlag, Berlin, 1984).

3. R Trommer, H Muller, M Cardona and P Vogl, *Phys. Rev.* **B21**, 4869 (1980).

4. K Strossner, S Ves, W Deterich, W Gebhurdt and M.Cardona *Solid State Commun.***56**, 563 (1985).

5. R Trommer, E Anastassakis and M Cardona, in *Light Scattering Solids*, edited by M Balkanski, R C C Leite, and S P S Porto (Flammarion, Paris, 1976) 396.

6. B A Weinstein, J B Renucci and M Cardona, *Solid State Commun.* **12**, 473 (1973).

7. B A Weinstein and C J Peirmarini, *Phys. Rev.* **B12**, 1172 (1975).

8. D Olego and M Cardona, *Phys. Rev.* **B25**, 1151 (1982).

9. D Olego, M Cardona and P Vogel, *Phys. Rev.* **B25**, 3878 (1982).

10. S Koltz, J M Besson, M Schwoerer-Bohning, R Nelmes, M Barden and L Pintschovius, *Appl. Phys. Lett.* **66**, 1557 (1995), S Koltz, J M Besson, G Hamel, R Nelmes, J S Loveday and W G Marshall, *High Pressure Research* **14**, 249 (1996).

11. L Pintschovius, *Nuclear Intrum. and methods* **A 338**, 136 (1994).

12. S Koltz, J M Besson, M Barden, K Karch, F Bechstedt, D Strauch and P Pavone, *Phys. Stat Sol.(b)* **180**, 100 (1996).

13. C Patel, W F Sherman and G R Wilkinson, *Phys. Stat Sol.(b)* **114**, 169 (1982).

14. S M Sharma and S K Sikka, *J.Phys. Chem. Solids* **46**, 477 (1985).

15. J K Jaffe, R Pandey and M J Seel, *Phys. Rev.* **B47**, 6299 (1993).

16. O H Nielsen and R M Martin *Phys. Rev.* **B32**, 3780 (1985), **32**, 3972 (1985).

17. P Rodriguez-Hernandez and A Munoz, *Semicond. Sci. Technol.***7**, 1437 (1992).

18. K Kunc, M Balkanski and M Nusimovici, *Phys. State Solidi (b)* **72**, 229, (1975).

19. R J Nelmes and M I Macmahon, *Semicond. Semimet.* **54**, 145 (1998) and references therein.

20. P Kicinski and M Zbroszczyk, *Semicond. Sci. Technol.* **10**, 1452 (1995).

21. G Dolling, In *Symposium on Inelastic Scattering of Neutron in Solids and liquids* (IAEA, Vienna 1963) Vol. **II**, 37, G Dolling and J L T Waugh, *Lattice Dynamics*, ed. R F Wallis, 19 (Pergamon Press, Oxford, 1965).

22. J L Yarnell, J L Warren R G Venzel and P J Dean , *in the fourth IAEA Symposium on Inelastic Neutron Scattering* (IAEA, Vienna 1968) Vol. **I**, 301.

23. M K Faar, J G Traylor and S K Sinha, *Phys. Rev.* **B 11,** 1587 (1975).

24. P H Borcherds, G F Alfrey, D.H. Saunderson and A.D.B. Woods, *J.Phys.* **C8**, 2022 (1975).

25. (a) N S Orlova, *Phys. Stat. Solidi (b)* **103**, 115 (1981), (b) R Charles, N Saint-Cricq, J B Renucci and A Zwick, *Phys. Rev.* **B 22,** 4804 (1980).

26. D L Price, J M Rowe and R M Nicklow, *Phys. Rev.* **B 3,** 1268 (1971).

27. D N Talwar, M Vandevyver, K Kunc and M Zigone . *Phys. Rev.* **B 24,**741 (1981).

28. J A Sanjuro, E Lopez-Cruz, P Vogl andM Cardona, *Phys. Rev.* **B 28,** 4579 (1983).

29. S Koltz, M Barden, J Kulda, P Pavone and B Steininger, *Phys. Stat. sol. (b)* 223, 441(2001).

30. S Froyen and M L Cohen *Phys. Rev.* **B28**, 3258 (1983).

31. J R Chelikowsky and S G Louie, *Phys. Rev.* **B29**, 3470 (1985).

32. R K Singh and Sadhna Singh, *Phys. Rev.* **B39**, 761 (1989).

33. G Alfrey and P A Borcherd, *J. Phys.*, **C5**, L275 (1972).

34. P A Borcherd, G Alfrey, D H Saunderson and A B B Woods, *J. Phys.* **C8**, 13, 2022 (1975).